Nuclear Magnetic Resonance

Ben Rasmussen
Department of Physics and Astronomy, University of Victoria
(Dated: December 5, 2023)

The fundamentals of pulsed nuclear magnetic resonance were explored in detail using a TeachSpin PS2 instrument. A sample of light mineral oil (LMO) was selected for its relative ease of magnetization as well as its abundance of resonant nuclear protons to investigate fundamental principles of pNMR. In doing so, values for both the spin-lattice relaxation time and spin-spin relaxation time for the sample were obtained and compared to literature. Using two methods, the spin-lattice timescale was found to be found to be $T_1^{zp} = 0.047 \pm 0.007s$ using the zero-point crossing method and $T_1^{fid} = 0.059 \pm 0.001s$ using a $180° - \tau - 90°$ pulse sequence. Both were in a similar range to found values but inconsistent with experimental uncertainty. The spin-spin relaxation time was found in three ways. The first, using a spin-echo technique, resulted in a value of $T_2^{se} = 0.0442 \pm 0.0004s$. Utilizing both a Carr-Purcell and Meiboom-Gill pulse sequence gave way to values of $T_2^{cp} = 0.039 \pm 0.001s$ and $T_2^{mg} = 0.039 \pm 0.001s$. These were found to be very similar to literature but ended up inconsistent with the provided uncertainty.

I. INTRODUCTION

Nuclear Magnetic Resonance is an experimental technique essential to research in the physical sciences. Developed independently by both Edward Purcell and Felix Block in 1946 [1], they utilized continuous radio-frequency (RF) signals to probe the magnetic properties of nuclei. The principles of pulsed NMR were later developed in 1950 by Erwin Hahn [1] incorporating bursts of RF signal used to observe transient effects on the magnetic nuclei inside of the sample [2]. The physical principles governing both methods are the same, leveraging spin properties of magnetic atoms to gain information and potentially image samples, however the advantages of a pulsed NMR setup have made it the standard. With applications in chemistry, biology, and medicine (MRI), nuclear magnetic resonance techniques are an important part of the scientific lexicon.

Theory:

To begin our analysis of magnetic compounds, we consider a semi-classical particle with non-zero angular momentum (necessary for magnetic resonance) as in [1]. The relationship between the angular momentum and magnetic moment is given by:

$$\vec{\mu} = \gamma \vec{I} \tag{1}$$

where $\gamma = \frac{g\mu_N}{\hbar} = \frac{ge}{2m_p}$ is the quantum mechanical gyromagnetic ratio and μ_N is the nuclear magneton. g here is the spectroscopic splitting factor [1]. For a proton, the g-factor is given by $g = 5.585694689 \pm 0.000000002$ [3].

Of particular interest to us is when this particle is placed into an external magnetic field $\vec{B}_0$. A torque acting on the particle will result in a change to the angular momentum as:

$$\vec{\tau} = \vec{\mu} \times \vec{B}_0 = \frac{d\vec{I}}{dt} = \frac{1}{\gamma}\frac{d\vec{\mu}}{dt} \tag{2}$$

Since the rate of change of $\vec{\mu}$ is always perpendicular to both $\vec{mu}$ and the external magnetic field, we will necessarily achieve processional motion around the direction of $\vec{B}_0$.

Now if we restrict our particle to a type with intrinsic angular momentum (spin) of $I = \frac{1}{2}$ such as protons, we notice a splitting of the ground state energies via quantum mechanics. Since our magnetic quantum number can occupy both $\pm\frac{1}{2}$ and the energy from the magnetic moment is given by:

$$U = -\vec{\mu}B_0 = -\mu_z B_0 = -\gamma\hbar m_I B_0 \tag{3}$$

We can see that there are two distinct lowest energies. In this case, we have taken only the z-direction projection, as the field is assumed to be along z. We can quantify the difference in energies of these two states as:

$$\Delta U = U_- - U_+ = \gamma\hbar B_0 \tag{4}$$

Where $U_\pm$ are the two states corresponding to the $m_I = \pm\frac{1}{2}$ spin states. It is then possible to imagine a transition between the high and lower spin states induced by a photon carrying ΔU energy, or:

$$\hbar\omega_0 = \gamma\hbar B_0 \tag{5}$$

which gives us: $\omega_0 = \gamma$ which is the Larmor frequency [4]. Specifically for protons, the gyromagnetic ratio is $\gamma = 2.675 \times 10^8 \frac{rads}{sT}$. After plugging in all values, we arrive at a required photon frequency of:

$$f_0(MHz) = 4.2577 \times B_0(kG) \tag{6}$$

In reality, samples will be made up of many, many such particles each exhibiting the above spin properties. It is

useful then to consider a *net* magnetization of the entire sample. As an example, the z-component will be given by:

$$M_z = \sum_i \gamma \hbar m_i = \frac{1}{2}\gamma\hbar(N_+ - N_-) \tag{7}$$

Where $N_\pm$ are the protons occupying the two states in the sample. As for other components, we will have that $M_x = \sum_i \mu_{xi}$. To generalize the magnetization dynamics in all three spatial dimensions, we can use the result from [5] as the phenomenological Bloch equations are:

$$\frac{d\vec{M}}{dt} = \gamma\vec{M} \times \vec{H} - \hat{x}\frac{M_x}{T_2} - \hat{y}\frac{M_y}{T_2} - \hat{z}\frac{M_z - M_0}{T_1} \tag{8}$$

Where $\vec{B} = \mu\vec{H}$ and T_1, T_2 are relaxation times that will be explored further.

The 90° *Pulse:*

Consider a sample of protons that has a net magnetization in the z-direction. If we apply an RF pulse at resonance with the sample for a specific duration A, such that the net spins in the sample are rotated from the z direction into the x-y plane, a signal can be generated in a spectrometer. In this experiment, spin dynamics are only measured with respect to the x-y plane and as such a value for A is optimized at the maximum signal value. If the RF pulse with duration A is successful at tilting a maximum amount of net magnetization into the transverse directions, we call this a 90° pulse as the net spins change at a right angle to the longitudinal magnetization. A 90° pulse will generate a signal with a maximum right after the pulse that decays as the x-y components re-establish equilibrium with the applied field. This is called the Free Induction Decay or FID.

The 180° *Pulse:*

In a similar way, a pulse may be applied to a sample such that the net magnetization of the sample is in opposition to the external magnetic field after the pulse. An optimized length of this pulse, B, results in a zero signal as spins are shifted from z to -z with net movement cancelling out in the x-y plane. This pulse is called a 180° pulse as the magnetization shifts are in opposite direction to the applied field. We may combine these pulses in sequences to calculate properties of the material in question.

Spin-Lattice Relaxation (T_1)*:*

The spin-lattice relaxation time, or T_1, is the characteristic timescale associated with the spins in the sample re-establishing thermal equilibrium magnetization with the z-direction [6]. To measure this value, as our spectrometer can only pick up signals in the x-y plane, we must apply a sequence of $180^\circ - \tau - 90^\circ$, where τ is the delay between pulse B and pulse A. This works to probe the M_z component of magnetization (or change thereof) as the first pulse tilts all spins into the -z direction which are then reoriented back into the x-y plane producing a FID. The amplitude of this FID is proportional to the M_z and as such will be a function of the time delay τ as it depends on how much of the spins have rephased into the +z direction from the initial pulse. In this regime, the M_Z component of magnetization dominates and we can use a simplified form of equation (8):

$$\frac{dM_z}{dt} = \frac{-(M_z - M_0)}{T_1} \tag{9}$$

Where M_0 is the equilibrium magnetization. We may solve this as:

$$\int \frac{dM_z}{(M_z - M_0)} = \int \frac{-dt}{T_1} \tag{10}$$

$$M_z = M_0 - Ae^{\frac{-t}{T_1}} \tag{11}$$

But our initial conditions after the first pulse must be $M_z(T = 0) = -M_0$ and so we arrive at the following:

$$M_z = M_0(1 - 2e^{\frac{-t}{T_1}}) \tag{12}$$

Now of course our signal in the spectrometer will be in volts and only proportional to M_Z but the quantity of interest here is T_1 so we may ignore conversions and fit the function to a plot of FID amplitude as a function of delay time to obtain T_1. The zero crossing time will also give us another estimate as we have that where $M_z = 0$:

$$T_1 = \frac{\tau}{ln(2)} \tag{13}$$

Spin-Spin Relaxation (T_2)*:*

The other relaxation time of interest is the time for spins to lose a non-thermal equilibrium state of x-y plane magnetization called the spin-spin relaxation, or T_2 [6]. The primary mechanism here is the dephasing of spins caused by their individual changes to the local magnetic field due to their procession frequency. If the field across the sample is inhomogeneous (as will be the case in any real-world experiment), it becomes difficult to probe this value as it will depend of the morphology of the field. To get around this, we may induce what is called a spin-echo. To do this, we apply a sequence of pulses as $90^\circ - \tau - 180^\circ$. After the first pulse, inducing a FID, the spins in a stronger field move quicker to equilibrate and vice versa. With the application of the

180° pulse, any spin that is ahead of the sequence now becomes behind with the opposite being true. As the spins return to equilibrium they momentarily rephase producing an echo signal. The amplitude of which is dependent on the delay between each pulse τ.

In this regime, the dominant magnetization is those in the x-y plane. We once again return to equation (8) to model the dynamics, ignoring the first term:

$$\frac{dM_{x,y}}{dt} = -\frac{M_{x,y}}{T_2} \tag{14}$$

With solution:

$$M_{x,y} = M_0 e^{-\frac{t}{T_2}} \tag{15}$$

To actually measure the value of T_2, we may take two routes. The first involves varying the delay time τ to generate a spin echo and record the amplitudes. Fitting this with equation (15) will yield a T_2 value. Using similar mechanisms, the decay of spin amplitudes with increasing delay time can be found using an arbitrarily long sequence of 180° pulses with a total sequences of:

$$90° - \tau - 180° - 2\tau - 180° - 2\tau - 180° - 2\tau...$$

This is known as the Carr-Purcell sequence and will produce N spin echoes with decaying amplitude for N 180° pulses. We assume, of course, that each 180° pulse is flips spins exactly that amount. This is not true in reality, and any phase error will accumulate over the course of the sequence. To improve on this, we use the Meiboom-Gill sequence that shifts the phase of the RF signal by 90° for the first pulse relative to the phase of the subsequent 180° pulses so that there is no accumulated phase error [1].

II. METHOD

To obtain data for this experiment, the TeachSpin PS2 Spectrometer was used in conjunction with a significant permanent magnet, temperature and magnetic field gradient controller, and an oscilloscope. Each component had a number of parameters that needed optimizing. For this specific experiment, the sample used was a light mineral oil which is easily magnetized and produces a clean signal.

The first step in calibrating the instrument was to impedance match the tuning capacitors. Using an RF sample probe, the capacitors in the magnet were adjusted so as to generate a peak-to-peak signal of about 40V during the RF pulses. The maximum obtained was $37.2V$.

The next major step was to achieve resonance between the samples natural procession frequency and the applied RF pulse. To do so, the env OUT bnc and the Q OUT bnc were attached to the oscilloscope. The Q output is the product of the processing spin signal times the oscillator reference signal [7] resulting in:

$$sin(\omega_{ref}t) \cdot sin(\omega_{spins}t) = \frac{1}{2}cos[(\omega_{ref} - \omega_{spins})t] - \frac{1}{2}cos[(\omega_{ref} + \omega_{spins})t]$$

The high frequency contribution from the second term is filtered out and we are left with a beat signal [7]. We may then adjust the frequency of the RF pulse to make this term go to zero. As can be seen in figure (1), an off resonance signal is very obvious. We may motivate a starting point for the frequency using equation (6) as we know the applied field should be $5kGauss$:

$$f_0(MHz) = 4.2577 \times 5 = 21.2885MHZ$$

Due to changes in the applied field, the value found for the light mineral oil (LMO) sample hovered around $f = 21.54283MHz$. This value had some drift associated with it, likely due to the temperature dependence of the apparatus components used. The instrument is equipped with a temperature control unit that allows for a field stability of $\pm 5x10^{-4}mT$ over a period of a quarter hour [7]. This was utilized in all experiments and allowed to stabilize for sufficient time before operation of the equipment.

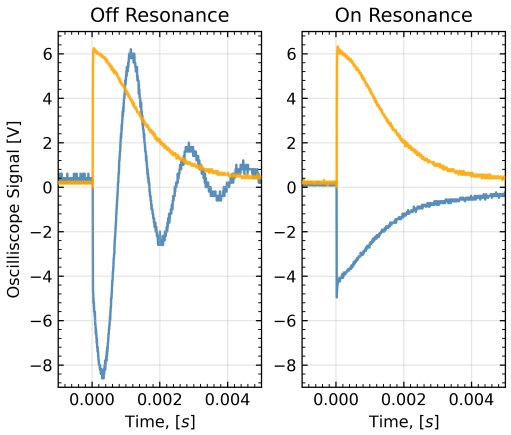

FIG. 1: Oscilloscope trace for the LMO sample detuned from resonance as well as optimized to obtain resonance between the oscillator frequency and the natural frequency of the spins in the sample. Rightmost plot is desired for all scenarios and was optimized before each experiment.

As described in section I, the strength of a free induction decay is dependent on a number of things including but not limited to the efficiency of the 90° pulse, the homogeneity of the applied magnet, and the strength of resonance outlined above. The first parameter varied was the length of the 90° pulse until a maximum was reached at a pulse length of $A = 4.20\mu s$.

A more homogeneous field results in a longer envelope of the FID [7]. To help with this are a number of magnetic field gradient coils. These were systematically adjusted starting in sequence of $\frac{\partial B_z}{B_x} \rightarrow \frac{\partial B_z}{B_y} \rightarrow \frac{\partial B_z}{B_z} \rightarrow \frac{\partial^2 B_z}{B_z^2}$ a sufficient number of times to obtain an optimal FID. The final values for the coils were $(x = 3.0, y = 5.8, z = 2.6, z^2 = 1.8)mm$ leading to a curve not unlike that shown in figure (2).

The final step in ensuring accurate results was the determination of an appropriate length for the 180° pulse. To do this, a 180° pulse was applied and adjusted until a near zero signal was obtained. This resulted in a value of $B = 10.20\mu s$.

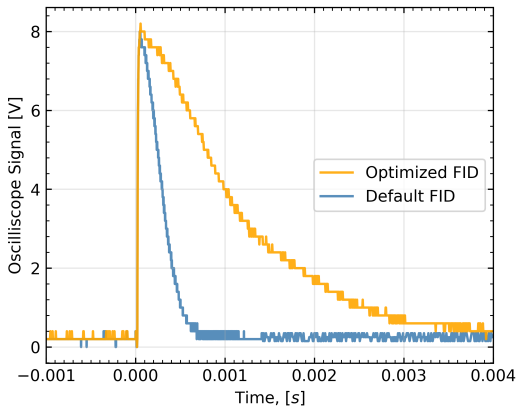

FIG. 2: Oscilliscope trace for the LMO sample taken before any cahnges were made to the apparatus parameters (Blue) and after optimization. Width of FID signal is a function of many parameters, including the length of the pulse applied (A) and the gradient field coil strengths (B_z, B_x, B_y, B_{z^2}).

III. RESULTS AND ANALYSIS

Determination of T_1:

We obtained two seperate values for the spin-lattice relaxation time. To do so, the FID amplitudes for a $180° - \tau - 90°$ sequence were recorded for varying values of τ. This produced a plot seen in figure (3). As signals from the instrument are only returned as an absolute value, we corrected for this by inverting all values before the zero-point crossing. At that point, we estimated a value for T_1 using equation (13) as:

$$T_1 = \frac{\tau}{ln2} = 0.047 \pm 0.007s$$

Where the uncertainty is from the range of possible crossing times. Utilizing equation (12), fitting the data gives a more accurate value of T_1 of 0.059 ± 0.001 where uncertainty is due to the covariance of the fitting parameters.

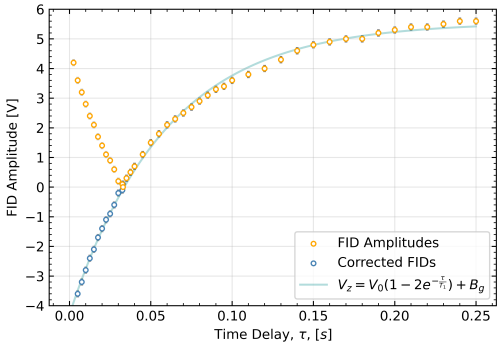

FIG. 3: FID amplitudes in a $180° - \tau - 90°$ sequence for LMO as a function of changing values of τ. z and -z magnetization components will both produce a positive signal so the small τ amplitudes have been corrected to fall below the x-axis. The resulting curve was fitted with the appropriate T_1 curve with $\chi^2 = 74.8$, $\nu = 41$, and a p-value = 0.993 confirming goodness-of-fit.

Determination of T_2:

Spin-Echo Amplitude Method:

We were able to find a value for the spin-spin relaxation time using three different methods. The first varied τ values in a $90° - \tau - 180°$ pulse sequence and measured the amplitudes of the spin-echo. The data can be seen in figure (4). The resulting value for T_2 was 0.0442 ± 0.0004 where uncertainty is from the fitting routine. Uncertainty on the data values themselves is due to the resolution of the oscilloscope.

Spin-Echo Sequences Methods:

Utilizing the sequence methods outlined in part I gives us a number of other values for T_2. The resulting oscilloscope trace from both the Carr-Purcell (CP) and Meiboom-Gill (MG) sequences can be seen in figure (5). The differences will be highlighted later on. We took five trials for each of the sequences and averaged the ith peak of the sequence. A value of τ that allowed for sufficient separation between peaks and resolution for almost all of the induced pulses was chosen to be $\tau = 0.0040s$. To get enough data points, we included 30 180° pulses.

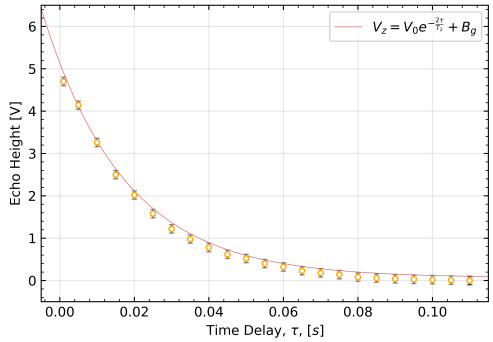

FIG. 4: Echo amplitudes in a $90° - \tau - 180°$ sequence for LMO as a function of changing values of τ. The resulting curve was fitted with the appropriate T_2 equation with $\chi^2 = 14.8$, $\nu = 22$, and a p-value = 0.870 confirming goodness-of-fit. Uncertainty from Oscilloscope tick resolution.

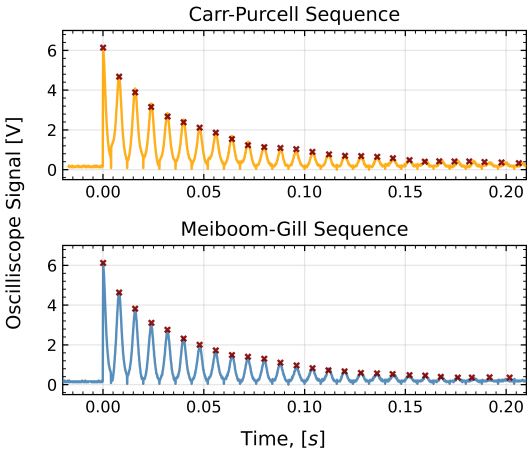

FIG. 5: Oscilloscope Trace for both the Carr-Purcell and Meiboom-Gill sequence with $A = 4.20\mu s$, $B = 10.20\mu s$, $\tau = 0.0040s$, and the number of 180° pulses as $N = 30$. Overlaid in red are the average local peak heights over 5 data runs.

Uncertainty for these values was due to the standard deviation from the ith pulse averaging. Using equation (15), we were able to fit these curves, giving two different values of T_2 for the CP and MG sequences of 0.039 ± 0.001 and 0.039 ± 0.001 respectively (not an error).

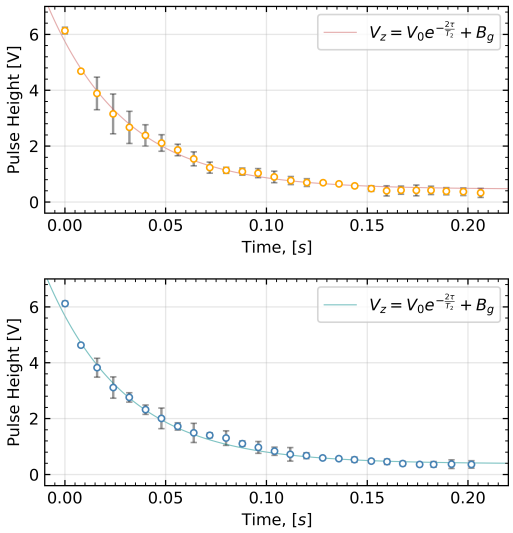

FIG. 6: Average Peak heights for both the Carr-Purcell and Meiboom-Gill sequence over 5 data runs as a function of time with $A = 4.20\mu s$, $B = 10.20\mu s$, $\tau = 0.0040s$, and the number of 180° pulses as $N = 30$. Uncertainty is from the standard deviations in ith peak over 5 data runs. Both sequences have been fitted with T_2 equation with $\chi^2_{cp} = 8.7$, $\nu_{cp} = 24$, and a p-value = 0.998 and $\chi^2_{mg} = 9.5$, $\nu_{mg} = 23$, and a p-value = 0.993 confirming goodness-of-fit in both cases.

IV. DISCUSSION

Investigations into the fundamental methods surrounding pulsed nuclear magnetic resonance were successfully undertaken in this experiment. Using a sample of light mineral oil, the spin-lattice relaxation time was determined to be $T_1 = 0.047 \pm 0.007s$ using the zero-point crossing method and $T_1 = 0.059 \pm 0.001s$ using a $180° - \tau - 90°$ pulse method. Literature suggests this value is $T_1 = 0.0573 \pm 0.0003s$ [8] which is very close but slightly inconsistent with the value found here in the second method. Uncertainty is primarily due to the oscilloscope resolution in this portion of the experiment. It would have been useful to take multiple trials of this measurement to get a better estimate of the true uncertainty as from the fit it seems like it may be underestimated.

The spin-spin relaxation time for LMO was found in three different ways. The first was a spin-echo experiment involving a $90° - \tau - 180°$ pulse sequence that yielded a value of $T_2^{se} = 0.0442 \pm 0.0004s$. Using both the Carr-Purcell and Meiboom-Gill pulse sequences, further values for T_2 were obtained. These were $T_2^{cp} = 0.039 \pm 0.001s$ and $T_2^{mg} = 0.039 \pm 0.001s$. From literature, a value for the a similar sampled was found to be $T_2 = 0.0376 \pm 0.0002s$. All three values are

very close to the found value but are inconsistent with the experimental uncertainty. Uncertainty in the first case is once again due to the oscilloscope resolution. However, in the second and third value it is provided due to the standard deviation from 5 samples. These values are the most consistent with the literature value.

Of note is the comparison between the two sequences. It is clear from figure (6) that the individual uncertainties on each point is higher for the CP sequence. We may also notice that in figure (5), the MG sequence achieves better separation between subsequent peaks and reaches a much better null value during the 180° pulses. This is expected as the MG sequence is an improvement on the CP. What is unexpected is that the values and fitted uncertainties are identical. Further, the goodness of fit test is actually better for that of the CP sequence. Over a more rigorous test this will likely not hold.

Much effort was spent on making the continuous wave NMR experiment work for this sample but was omitted from the theory and analysis for the sake of brevity since no significant results were obtained before December 4th. Further work on this project will necessarily involve getting a consistent signal for a continuous wave stimulus not just RF pulses. As the foundations of the instrument and principles of operation are well understood, extensions to this include finding similar properties for more exotic samples in the future.

V. CONCLUSION

In this experiment, the principles of pulsed nuclear magnetic resonance were demonstrated on a light mineral oil sample, allowing for multiple determinations of the spin-lattice relaxation time and the spin-spin relaxation time. The T_1 values were found to be $T_1^{zp} = 0.047 \pm 0.007s$ using the zero-point crossing method and $T_1^{fid} = 0.059 \pm 0.001s$ using a $180° - \tau - 90°$ pulse sequence. Both were found to be in the ballpark of literature values but inconsistent with the provided uncertainty. As for the spin-spin relaxation for light mineral oil, three values were found. The first, using a spin-echo technique, resulted in a value of $T_2^{se} = 0.0442 \pm 0.0004s$. Using both a Carr-Purcell sequence and a Meiboom-Gill sequence, the values were found to be $T_2^{cp} = 0.039 \pm 0.001s$ and $T_2^{mg} = 0.039 \pm 0.001s$. These were both very close but ultimately inconsistent with found values in literature.

[1] R. V. D. J. Stoltenberg, D. Pengra, "Pulsed nuclear magnetic resonance," (2006).

[2] TeachSpin, *Pulsed Nuclear Magnetic Spectrometer*, TeachSpin, Inc (1997).

[3] N. I. of Standards and Technology, `https://physics.nist.gov/cgi-bin/cuu/Value?gp` (2018), [Accessed: 3-December-2023].

[4] E. P. Wagner, "Understanding precessional frequency, spin-lattice and spin-spin interactions in pulsed nuclear magnetic resonance spectroscopy," (2014).

[5] J. W. David Stephen, Tao Fang, "Physical principles of nuclear magnetic resonance and applications," (2016).

[6] B. Wolff-Reichert, "Conceptual tour of pulsed nmr," (2008).

[7] TeachSpin, *Pulsed/CW NMR Spectrometer*, TeachSpin, Inc (2013).

[8] H. S. Will Weigand, Adam Egbert, "Determining the relaxation times, t1,t2, and t*2 in glycerin using pulsed magnetic resonance," (2015).

APPENDIX A: Fitting Parameters

TABLE I: Model and fitting parameters for instances of fitting found in figures:

	Spin-Lattice Relaxation Time	$V_z(M_z) = V_0(M_0)(1 - 2e^{\frac{\tau}{T_1}}) + B_g$	
	V_0 [Volts]	T_1 $[s]$	B_g [Volts]
T_1 Determination	(4.93 ± 0.03)	(0.0588 ± 0.001)	0.63 ± 0.05
	Spin-Spin Relaxation Times	$V_z(M_z) = V_0(M_0)e^{\frac{\tau}{T_1 2}} + B_g$	
	V_0 [Volts]	T_2 $[s]$	B_g [Volts]
Spin Echo Amplitude Method	(5.07 ± 0.03)	(0.0442 ± 0.0004)	(0.0064 ± 0.007)
Carr-Purcell Sequence	(5.29 ± 0.03)	(0.039 ± 0.001)	(0.45 ± 0.02)
Meiboom-Gill Sequence	(5.30 ± 0.02)	(0.039 ± 0.001)	$(0.38 \pm 0.0.02)$